

# Degenerate Swin to Win: Plain Window-based Transformer without Sophisticated Operations

Tan Yu, Ping Li

Cognitive Computing Lab  
Baidu Research  
10900 NE 8th St. Bellevue, WA 98004, USA

{tan.yu1503, pingli98}@gmail.com

## Abstract

The formidable accomplishment of Transformers in natural language processing has motivated the researchers in the computer vision community to build Vision Transformers. Compared with the Convolution Neural Networks (CNN), a Vision Transformer has a larger receptive field which is capable of characterizing the long-range dependencies. Nevertheless, the large receptive field of Vision Transformer is accompanied by the huge computational cost. To boost efficiency, the window-based Vision Transformers emerge. They crop an image into several local windows, and the self-attention is conducted within each window. To bring back the global receptive field, window-based Vision Transformers have devoted a lot of efforts to achieving cross-window communications by developing several sophisticated operations. In this work, we check the necessity of the key design element of Swin Transformer, the shifted window partitioning. We discover that a simple depthwise convolution is sufficient for achieving effective cross-window communications. Specifically, with the existence of the depthwise convolution, the shifted window configuration in Swin Transformer cannot lead to an additional performance improvement. Thus, we degenerate the Swin Transformer to a plain Window-based (Win) Transformer by discarding sophisticated shifted window partitioning. The proposed Win Transformer is conceptually simpler and easier for implementation than Swin Transformer. Meanwhile, our Win Transformer achieves consistently superior performance than Swin Transformer on multiple computer vision tasks, including image recognition, semantic segmentation, and object detection.

# 1 Introduction

Recently, the triumph achieved by Transformer (Vaswani et al., 2017) in natural language processing, some works attempt to deploy Transformer in computer vision applications and built Vision Transformers (Dosovitskiy et al., 2021; Touvron et al., 2021a; Han et al.). Compared with convolutional neural networks (Krizhevsky et al., 2012; He et al., 2016), a Vision Transformer has a larger receptive field, effectively capturing the long-range relations between pixels. Meanwhile, different from convolution layer processing images by a static convolution kernel, the self-attention operations in Vision Transformer are dynamic, which effectively model the relations in the image adaptively. Nevertheless, the powerful representing capacity of the self-attention operations in Vision Transformers is accompanied by the potential efficiency issue. To be specific, the computational complexity of a self-attention operation is proportional to the square of the number of tokens. Thus, only a limited number of tokens can be allowed in the self-attention operation to achieve satisfactory efficiency. The pioneering works, ViT (Dosovitskiy et al., 2021) and DeiT (Touvron et al., 2021a), considering the efficiency, have to partition an image into a low-resolution feature map consisting of only  $16 \times 16$  patches/tokens. Nevertheless, the coarsely partitioned low-resolution feature map limits Vision Transformers’ capability in visual understanding, especially for dense prediction tasks such as segmentation.

For effective dense prediction and acceptable efficiency, Pyramid Vision Transformer (PVT) (Wang et al., 2021), Pooling-based Vision Transformer (PiT) (Heo et al., 2021) and Hierarchical Visual Transformer (HVT) (Pan et al., 2021) design a high-resolution feature map in the initial layer and reduces the resolution in deep layers with a progressive shrinking pyramid structure. In parallel to the pyramid structure, window-based local attention is another widely used manner for improving efficiency. Swin Transformer (Liu et al., 2021) crops an image into non-overlapping windows, and the self-attention is exploited within each window. In spite of improving efficiency considerably, the attention within the window constraints that a patch can only perceive the patches within the same window. The limited perceptive field impedes the communications between patches from different windows and might deteriorate understanding capability for long-range relations. To enable cross-window communication, Swin Transformer devises a shifted window partitioning mechanism. It adopts different manners for window partitioning in two consecutive layers, and the receptive field of each patch is enlarged. Similarly, Twins (Chu et al., 2021) and Shuffle Transformer (Huang et al., 2021) also adopt the window-based local attention for high efficiency and devote a lot of effort to bringing back the global receptive field for high effectiveness. Specifically, Twins (Chu et al., 2021) develops global sub-sampled attention, which is with global receptive field and complements window-based local attention. In a similar manner, Shuffle Transformer develops a shuffled local-window attention module, which is complementary to the vanilla window-based local attention.

In this work, we check the necessity of the sophisticated operation, shifted window partitioning, for bringing back the global receptive field proposed in Swin (Liu et al., 2021). To differentiate from the shifted window-based local attention, we term the vanilla window-based local attention without shifting as plain window-based local attention. Surprisingly, we discover that, after pairing a plain window-based local attention layer with a simple depthwise convolution, it has consistently better performance than Swin Transformer in image recognition, semantic segmentation, and object detection. Meanwhile, with the existence of depthwise convolutions, the shifted window partitioning in Swin can not bring additional performance improvement. Thus, we degenerate Swin to a plain Window-attention Transformer (Win), which is conceptually simpler than Swin, Twins, and Shuffle Transformer. Specifically, we have removed quite a few lines of code in Swin Transformer. Meanwhile, our Win Transformer achieves competitive performance in image recognition, object detection,

and semantic segmentation. Compared with previous Vision Transformers, the proposed Win Transformer does not contain any sophisticated operations. On the contrary, it removes some redundant operations. Taking the simplicity, the efficiency, and the effectiveness into consideration, our Win Transformer is a good choice for real applications.

## 2 Related Work

**Self-attention mechanism in CNN.** In the past decade, the convolutional neural network (CNN) (LeCun et al., 1995; Krizhevsky et al., 2012; He et al., 2016) has been *de facto* backbone for vision understanding. The local receptive field of the convolution layer limits its capability of capturing the long-range dependencies. Thus, there are many works attempting to improve the performance of CNN through introducing the self-attention operation. Non-local neural network (Wang et al., 2018) is one of the earliest works to plug self-attention modules in CNNs for video understanding. Since the long-range dependencies are important for video recognition, self-attention is considerably helpful in this scenario. Cao et al. (2019); Yin et al. (2020) further investigate the non-local neural network in depth and apply it in various image understanding tasks such as semantic segmentation and object detection. Attention Augmented Convolutional Network (Bello et al., 2019) builds a hybrid architecture by replacing a few convolution layers with self-attention layers. It augments a convolution with the self-attention mechanism. DETR (Carion et al., 2020) builds an encoder-decoder Transformer architecture to post-process the feature map from a CNN for the object detection task. Similarly, Relationnet++ (Chi et al., 2020) builds an object detector through Transformer decoder. Deformable DETR (Zhu et al., 2021) improves the training efficiency and detection accuracy of DETR by an iterative bounding box refinement mechanism. SETR (Zheng et al., 2021) adopts ViT (Dosovitskiy et al., 2021) as encoder and incorporates CNN decoders to inflate the feature resolution. BoTNet (Srinivas et al., 2021) replaces the convolutions with global self-attention in the last a few bottleneck blocks of a ResNet, achieving outstanding performance in image recognition.

**Global-attention Vision Transformer.** ViT (Dosovitskiy et al., 2021) builds the first pure Transformer architecture for computer vision tasks. It tokenizes an image by cropping an image into  $16 \times 16$  patches/tokens and builds a pure Transformer-based architecture to process the tokens for image recognition. DeiT (Touvron et al., 2021a) improves the data efficiency of ViT by introducing more advanced data augmentation and regularization methods. Due to the self-attention operations' quadratic complexity with respect to the number of tokens, ViT and DeiT can only adopt the low-resolution feature map, limiting their performance for dense prediction. PVT (Wang et al., 2021) improves the performance of Vision Transformers for dense prediction by adopting a high-resolution feature map. To alleviate the high computational cost issue in a high-resolution feature map, PVT learns from the design of the convolutional neural network and builds a hierarchical pyramid structure, progressively reducing the resolution to boost efficiency. PiT (Heo et al., 2021) and HVT (Pan et al., 2021) conduct pooling to shrink the spatial dimension and inflates the channel dimension gradually for achieving high efficiency and effectiveness. Similarly, Multi-scale Vision Transformer (Fan et al., 2021) hierarchically expands the channel capacity while reducing the spatial resolution. Segformer (Xie et al., 2021) adopts the hierarchically structured Transformer encoder which outputs multi-scale features for effective semantic segmentation. Tokens-to-Token ViT (Yuan et al., 2021) recursively aggregates neighboring tokens into one token to model the local structure and progressively reduces the token length. Transformer in Transformer (TNT) (Han et al., 2021a) models the attention inside these local patches to boost the performance further.

CaiT (Touvron et al., 2021b) and DeepViT (Zhou et al., 2021) investigate in deeper Transformer for achieving higher recognition accuracy. Convolutional vision Transformer (CvT) (Wu et al., 2021) introduces convolutions to capture local spatial context and reduce semantic ambiguity in the attention mechanism. LeViT (Graham et al., 2021), Early Convolutions (Xiao et al., 2021), Uniformer (Li et al., 2022) and LIT (Pan et al., 2022) adopt convolutions/MLPs in early stages to improve Vision Transformers’ efficiency and effectiveness.

**Local-attention Vision Transformer.** To further improve efficiency, some recent works (Liu et al., 2021; Chu et al., 2021; Huang et al., 2021) exploit window-based local attention. They only exploit the self-attention operation within each local window individually, and the computational burden is alleviated. Nevertheless, window-based local attention impedes the communications between patches located in different windows and thus discards the long-range dependencies. To overcome the drawbacks inherited in window-based local attention, Swin Transformer (Liu et al., 2021), Twins (Chu et al., 2021), and Shuffle Transformer (Huang et al., 2021) adopt a dual-block architecture. That is, for consecutive two blocks, the first block adopts the window-based local attention, and the second one attempts to achieve the cross-window communications. To be specific, Swin Transformer (Liu et al., 2021) adopts the shifted window partition in the second block. Twins (Chu et al., 2021) devises global sub-sampled attention in the second block. The global sub-sampled attention block down-samples the global feature map into a low-resolution feature map to achieve a global receptive field in a lightweight manner. Shuffle Transformer (Huang et al., 2021) designs a spatial shuffle operation into the second window-based self-attention block for building connections among windows. Different from the dual-block architecture achieving the large receptive field through a cascade of two complementary blocks, recent Vision Transformers (Yang et al., 2021; Dong et al., 2021) put efforts on achieving the satisfactory receptive field within every single block in a parallel manner. Specifically, in Focal Transformer (Yang et al., 2021), a patch attends its closest surroundings in the same local window. In the meanwhile, it also sparsely sub-samples patches far from the patch as complementary information. CSWin (Dong et al., 2021) computes self-attention in the horizontal and vertical stripes in parallel and forms a cross-shape window. DW-S Conv (Han et al., 2021b) attempts to replace the self-attention operations in the local Vision Transformer with cheaper dynamic depthwise convolution, achieving comparable performance. BOAT (Yu et al., 2022b) exploits the feature-space local attention to boost the local-attention vision Transformer. MVT (Chen et al., 2021) utilizes the locality in projected view and proposed a local-global structure for effective and efficient 3D object recognition.

**Applications of Transformer at Baidu.** At Baidu, transformer and related techniques have been widely applied for (e.g.,) advertising, especially image/video advertising, including multi-modal/cross-modal retrieval for advertising (Yu et al., 2020, 2021b,a, 2022a). With the widespread use of transformer and other popular models in production, the issue of transformer-related model security has become an urgent matter. Therefore, recently there have been major efforts at Baidu for developing techniques for AI model security (Doan et al., 2021b,a, 2022).

### 3 Plain Window-attention Vision Transformer

**Overall architecture.** Following the previous works, Swin Transformer (Liu et al., 2021) and Shuffle Transformer (Huang et al., 2021), the proposed plain Window-attention (Win) Transformer also adopts a hierarchical pyramid structure consisting of four stages as visualized in Figure 1.

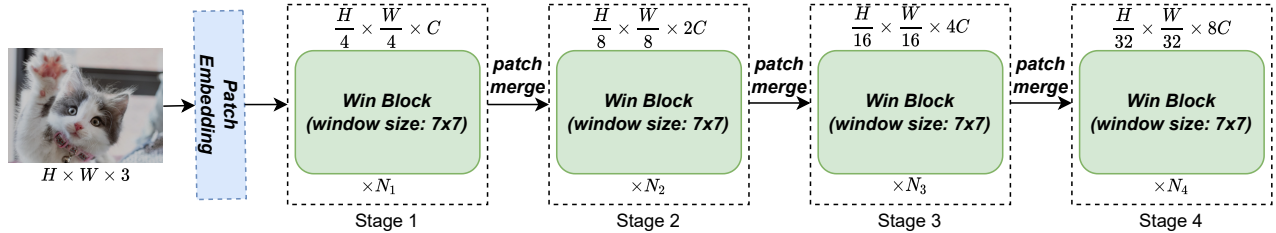


Figure 1: The architecture of the proposed plain Window-attention (Win) Transformer. It adopts a hierarchical pyramid structure with four stages.

Given an image of  $H \times W \times C$  size, a patch embedding layer generates the initial feature map of  $\frac{H}{4} \times \frac{W}{4} \times C$  size. Between consecutive two stages, there is a patch merging layer to reduce to half the width/height of the feature map and increases the channel dimension by 2. To be specific, in the  $i$ -th stage, the feature map is of  $\frac{W}{2^{i+1}} \times \frac{H}{2^{i+1}} \times 2^{i-1}C$  size. Each stage consists of a stack of the proposed Window-attention (Win) Block.

**Patch embedding and merging.** The patch embedding module converts a raw image into a feature map for further processing. Following Swin (Liu et al., 2021), in the patch embedding module, it crops an image into  $4 \times 4$  non-overlapped patches. A fully-connected layer projects each  $4 \times 4$  patches with 3 channels into a  $C$ -dimension vector. Between two consecutive stages, we plug in a patch merging module to reduce the spatial resolution and increase the channel number. Given a  $W \times H \times C$  feature map in the input, the output of the patch merging is of  $\frac{H}{2} \times \frac{W}{2} \times D$  size. Similar to Swin (Liu et al., 2021), the patch merging module concatenates the features of each group of  $2 \times 2$   $D$ -dimension patch features into a  $4D$ -dimension feature vector and further projects it into a  $2D$ -dimension vector.

**Window-attention (Win) block.** As shown in Figure 2, a Win block is built upon several layer-normalization (LN) layers (Ba et al., 2016), a window-based self-attention (WSA) module, an MLP module, a depthwise convolution (DConv) layer, and several skip connections. Given an input

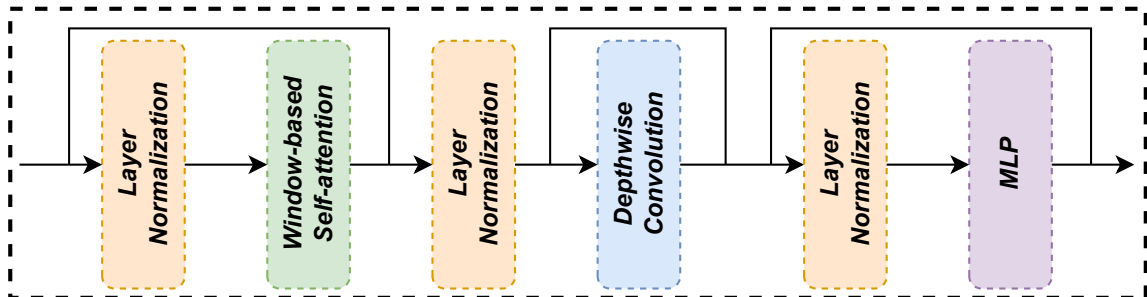


Figure 2: The Window-attention (Win) block consists of a window-based self-attention module, a depthwise convolution layer, an MLP module, and several layer-normalization layers.

feature map  $\mathcal{X} \in \mathbb{R}^{h \times w \times c}$ , it obtains the output  $\mathcal{Y}$  by conducting the below operations sequentially:

$$\begin{aligned} \mathcal{Y} &\leftarrow \mathcal{X} + \text{WSA}(\text{LN}(\mathcal{X})), \\ \mathcal{Y} &\leftarrow \text{LN}(\mathcal{Y}) + \text{DConv}(\text{LN}(\mathcal{Y})), \\ \mathcal{Y} &\leftarrow \mathcal{Y} + \text{MLP}(\text{LN}(\mathcal{Y})). \end{aligned} \tag{1}$$

The WSA module adopts the same setting as Swin (Liu et al., 2021) which uniformly partitions each feature map into non-overlapping  $7 \times 7$  windows. The multi-head self-attention operation is conducted within each  $7 \times 7$  local window. In the meanwhile, we add a position encoding operation in the window-based self-attention layer. We have attempted two types of position encoding, including the relative positional encoding (RPE) used in Swin (Liu et al., 2021) and locally-enhanced positional encoding (LEPE) in CSWin (Dong et al., 2021). The experiments show that RPE can perform slightly better than LEPE in image recognition on the ImageNet1K dataset. In contrast, for the downstream tasks such as semantic segmentation and object detection, LEPE performs slightly better than RPE. By default, we adopt LEPE on all experiments. To achieve the cross-window communications, we simply add a depth-wise convolution with a layer normalization and a residual connection after the window-based self-attention layer. The kernel size of the depthwise convolution is  $7 \times 7$ . The MLP module consists of two fully-connected layers with a GELU activation layer between them. The first fully-connected layer inflates the channel number of each patch from  $C$  to  $rC$ , and the second MLP layer shrinks the channel number from  $rC$  back to  $C$ , where  $r > 1$  is the inflation ratio. By default, we set  $r = 4$  in all settings, following Swin Transformers.

**Discussion.** Our Win Block can be regarded as a Swin Block without shifting. The only add-on module is a depthwise convolution, and our Win block does not conduct any novel and sophisticated operations. We attempt three types of ways to incorporate the depthwise convolution as visualized in Figure 3.

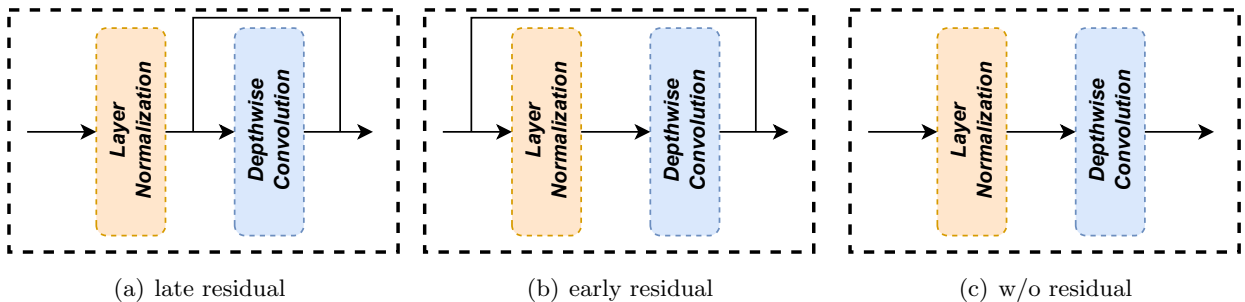


Figure 3: Three different approaches for incorporating the depthwise convolution.

Our experiments show the late-residual manner in Figure 3 (a) achieves the best performance. Actually, the manner of integrating depthwise convolution has a considerable influence on the model performance. Through extensive experiments, we discover that the simple depthwise convolution is sufficient for effective cross-window communications. With the existence of depthwise convolutions, sophisticated operations such as the shifted window partitioning in Swin Transformer can not bring further performance improvement. In fact, depthwise convolutions have been exploited in Shuffle Transformer to boost the model’s performance. Nevertheless, Shuffle Transformer uses depthwise convolutions to complement the shuffled window attention for cross-window communication. In contrast, our Win Transformer only uses the plain local window attention and solely relies on the depthwise convolution for cross-window communications. Moreover, Shuffle Transformer adopts the early-residual manner as shown in Figure 3 (b). Our experiments show that the early-residual manner can not achieve an excellent performance as the late-residual manner in our Win Transformer.

**Complexity analysis.** Due to using an additional depthwise convolution, our Win block takes slightly fewer parameters and more FLOPs than the Swin block. But the depthwise convolution is a very lightweight operation, which takes only a small number of parameters and FLOPs. We denote the channel number by  $c$ , the spatial size of the depthwise convolution kernel by  $k \times k$ , and the spatial size of the feature map size by  $H \times W$ . In this case, the depthwise convolution only takes  $k^2c$  parameters and  $WHk^2c$  FLOPs, which are marginal with respect to the total number of parameters and FLOPs of a Vision Transformer block.

## 4 Experiments

Following Swin (Liu et al., 2021), we built three types of backbones, including the tiny model (Win-T), the small model (Win-S), and the base model (Win-B). We illustrate the detailed configurations of them in Table 1. They adopt similar architectures as their Swin counterparts. Compared with Swin, our Win takes slightly more parameters and FLOPs. The marginal increases in the number of parameters and FLOPs are contributed to the lightweight depthwise convolution. The backbones are pre-trained on ImageNet-1K datasets without external data and are further fine-tuned on downstream tasks such as semantic segmentation and object detection.

Table 1: The configurations of Win-T, Win-S, and Win-B models.  $c$  denotes the channel number and  $h$  denotes the head number in self-attention operation.

| Stage      | Size           | Win-T                          | Win-S                           | Win-B                           |
|------------|----------------|--------------------------------|---------------------------------|---------------------------------|
| 1          | $56 \times 56$ | $\{c = 96, h = 3\} \times 2$   | $\{c = 96, h = 3\} \times 2$    | $\{c = 128, h = 4\} \times 2$   |
| 2          | $28 \times 28$ | $\{c = 192, h = 6\} \times 2$  | $\{c = 192, h = 6\} \times 2$   | $\{c = 256, h = 8\} \times 2$   |
| 3          | $14 \times 14$ | $\{c = 384, h = 12\} \times 6$ | $\{c = 384, h = 12\} \times 18$ | $\{c = 512, h = 16\} \times 18$ |
| 4          | $7 \times 7$   | $\{c = 768, h = 24\} \times 2$ | $\{c = 768, h = 24\} \times 2$  | $\{c = 1024, h = 32\} \times 2$ |
| Parameters |                | 29 M                           | 50 M                            | 88 M                            |
| FLOPs      |                | 4.5 G                          | 8.8 G                           | 15.6 G                          |

### 4.1 Image classification

**Settings.** We train the proposed Win Transformer on ImageNet1K dataset with 1.28 million training images and 50 thousand images for validation from 1,000 classes. Following DeiT (Touvron et al., 2021a) and Swin (Liu et al., 2021), we adopt AdamW (Loshchilov and Hutter, 2019) optimizer and train our models for 300 epochs using a cosine decay learning rate scheduler. We also conduct linear warm-up for the first 20 epochs. We set the batch size as 1024, the initial learning rate as 0.001, and the weight decay as 0.05. Following Swin, we adopt several data augmentation and regularization methods including RandAugment (Cubuk et al., 2020), Mixup (Zhang et al., 2018), Cutmix (Yun et al., 2019), random erasing (Zhong et al., 2020) and stochastic depth (Huang et al., 2016). We do not use repeated augmentation (Hoffer et al., 2020) and Exponential Moving Average (EMA) (Polyak and Juditsky, 1992), either. We set the stochastic depth with a ratio of 0.1, 0.3, 0.5 for Win-T, Win-S, and Win-B, respectively.

**Comparisons with existing methods.** To demonstrate the effectiveness of the proposed Win in the image recognition task, we compare it with a representative convolution neural network, ReGNet (Radosavovic et al., 2020), and other Vision Transformers, including DeiT (Touvron et al., 2021a), PVT (Wang et al., 2021), PiT (Heo et al., 2021), T2T (Yuan et al., 2021), Swin

Table 2: Comparisons with convolutional neural networks and other Vision Transformers on ImageNet-1K image classification.

| Method                                | Input Size | Params. (M) | FLOPs (G) | Top-1 Acc. (%) |
|---------------------------------------|------------|-------------|-----------|----------------|
| ReGNetY-4G (Radosavovic et al., 2020) | 224        | 21          | 4.0       | 80.0           |
| ConvNeXt-T (Liu et al., 2022)         | 224        | 29          | 4.5       | 82.1           |
| DeiT-S (Touvron et al., 2021a)        | 224        | 22          | 4.6       | 79.8           |
| PVT-S (Wang et al., 2021)             | 224        | 25          | 3.8       | 79.8           |
| PiT-S (Heo et al., 2021)              | 224        | 24          | 2.9       | 80.9           |
| T2T-14 (Yuan et al., 2021)            | 224        | 22          | 5.2       | 81.5           |
| TNT-S (Han et al., 2021a)             | 224        | 24          | 5.2       | 81.3           |
| Swin-T (Liu et al., 2021)             | 224        | 29          | 4.5       | 81.3           |
| Shuffle-T (Huang et al., 2021)        | 224        | 29          | 4.6       | 82.5           |
| NesT-T (Zhang et al., 2022)           | 224        | 17          | 5.8       | 81.5           |
| Focal-T (Yang et al., 2021)           | 224        | 29          | 4.9       | 82.2           |
| CrossFormer-S (Wang et al., 2022)     | 224        | 31          | 4.9       | 82.5           |
| CSWin-T (Dong et al., 2021)           | 224        | 23          | 4.3       | <b>82.7</b>    |
| Win-T (ours)                          | 224        | 29          | 4.6       | 82.3           |
| ReGNetY-8G (Radosavovic et al., 2020) | 224        | 39          | 8.0       | 81.7           |
| ConvNeXt-T (Liu et al., 2022)         | 224        | 50          | 8.7       | 83.1           |
| PVT-L (Wang et al., 2021)             | 224        | 61          | 9.8       | 81.7           |
| T2T-19 (Yuan et al., 2021)            | 224        | 39          | 8.9       | 81.9           |
| MViT-B (Fan et al., 2021)             | 224        | 37          | 7.8       | 83.0           |
| Swin-S (Liu et al., 2021)             | 224        | 50          | 8.7       | 83.0           |
| Twins-B (Chu et al., 2021)            | 224        | 56          | 8.3       | 83.2           |
| Shuffle-S (Huang et al., 2021)        | 224        | 50          | 8.9       | 83.5           |
| NesT-S (Zhang et al., 2022)           | 224        | 38          | 10.4      | 83.3           |
| Focal-S (Yang et al., 2021)           | 224        | 51          | 9.1       | 83.5           |
| CrossFormer-B (Wang et al., 2022)     | 224        | 52          | 9.2       | 83.4           |
| CSWin-S (Dong et al., 2021)           | 224        | 35          | 6.9       | 83.6           |
| Win-S (ours)                          | 224        | 50          | 8.9       | <b>83.7</b>    |
| ConvNeXt-B (Liu et al., 2022)         | 224        | 89          | 15.4      | 83.8           |
| DeiT-B (Touvron et al., 2021a)        | 384        | 86          | 55.4      | 83.1           |
| DeiT-B (Touvron et al., 2021a)        | 224        | 86          | 17.5      | 81.8           |
| PiT-B (Heo et al., 2021)              | 224        | 74          | 12.5      | 82.0           |
| Swin-B (Liu et al., 2021)             | 224        | 88          | 15.4      | 83.5           |
| Twins-L (Chu et al., 2021)            | 224        | 99          | 14.8      | 83.7           |
| Shuffle-B (Huang et al., 2021)        | 224        | 88          | 15.6      | 84.0           |
| NesT-B (Zhang et al., 2022)           | 224        | 68          | 17.9      | 83.8           |
| Focal-B (Yang et al., 2021)           | 224        | 90          | 16.0      | 83.8           |
| CrossFormer-L (Wang et al., 2022)     | 224        | 92          | 16.1      | 84.0           |
| CSWin-B (Dong et al., 2021)           | 224        | 78          | 15.0      | <b>84.2</b>    |
| Win-B (ours)                          | 224        | 88          | 15.6      | 83.5           |

Transformer (Liu et al., 2021), Shuffle Transformer (Huang et al., 2021), NesT (Zhang et al., 2022), Focal Transformer (Yang et al., 2021), CrossFormer (Wang et al., 2022), and CSWin Transformer (Dong et al., 2021). As shown in Table 2, using comparable number of parameters and FLOPs, our Win-T, Win-S, and Win-B achieve competitive performance compared with their counterparts. Especially, our Win-S achieves the best performance among all small-scale models. Note that our Win Transformers do not contain any sophisticated operations and are simply built upon the plain window-based self-attention layers, depthwise convolution layers, and MLP layers. In contrast, the compared counterparts devise several sophisticated operations, which are more complicated. It is considerably more difficult to implement them compared with ours. Note that, as shown in Table 2, our medium-scale model, Win-B, performs a little bit worse than the smaller counterpart, Win-S. The worse performance might be due to over-fitting.

**The manner of integrating depthwise convolution.** We evaluate the performance of different manners for integrating depthwise convolution. We compare three manners as visualized in Figure 3, including late residual connection in Figure 3 (a), early residual connection in Figure 3 (b), and w/o residual connection in Figure 3 (c). As shown in Table 3, the late residual connection achieves the best performance. Besides, after removing the residual connections, the performance considerably deteriorates. In the meanwhile, we observe from the table that, the advantage of the last residual connection over the early residual connection is more significant as the model capacity increases.

Table 3: The performance of different manners for integrating depthwise convolution. We report the top-1 accuracy of image recognition on ImageNet-1K dataset.

| Model | late residual | early residual | w/o residual |
|-------|---------------|----------------|--------------|
| Win-T | 82.3          | 82.2           | 82.1         |
| Win-S | 83.7          | 83.3           | 83.0         |
| Win-B | 83.5          | 83.1           | 83.0         |

**Depthwise convolution and shifted window partitioning.** We use depthwise convolution for achieving cross-window communication. In contrast, Swin adopts the shifted window partitioning for communications between patches from different local windows. Here, we evaluate effectiveness of depthwise convolution in our Win and the shifted window partitioning in Swin.

Table 4: The influence of depthwise convolution and shifted window partitioning. We report the top-1 accuracy of image recognition on ImageNet-1K dataset.

| Depthwise Conv |      | ✓    | ✓    |      |
|----------------|------|------|------|------|
| Shifted Window |      | ✓    | ✓    |      |
| Win-T          | 81.1 | 81.3 | 82.3 | 82.2 |
| Win-S          | 82.3 | 83.0 | 83.7 | 83.7 |

As shown in Table 4, by removing both depthwise convolution and shifted window partitioning, Win-Tiny as well as Win-Small cannot achieve a satisfactory image recognition performance. The low recognition accuracy is due to a lack of cross-window communication. After adopting the depthwise convolution or shifted window partitioning to achieve cross-window communication, the image recognition performance gets improved consistently for both Win-Tiny and Win-Small models. Table 4 illustrates that the depthwise convolution is more effective than the shifted window partitioning, and it achieves a considerably higher image recognition accuracy. In the meanwhile,

with the existence of the depthwise convolution, the shifted window partition can not bring further performance improvement. Therefore, we do not adopt the shifted window partitioning in our Win and just adopt the plain local window partitioning.

**The kernel size of depthwise convolution.** We evaluate the influence of the kernel size of the depthwise convolution. We vary the kernel size among  $\{3 \times 3, 5 \times 5, 7 \times 7\}$ . Our experiments in Table 5 shows that, the Win-Tiny model using a depthwise convolution with only  $3 \times 3$  spatial size has achieved excellent performance on image recognition. When the spatial size increases from  $3 \times 3$  to  $7 \times 7$ , the performance slightly improves. In the meanwhile, as the spatial size of the depthwise increases, the number of parameters and FLOPs also increase. Since the increase in the number of parameters and FLOPs is marginal, we set the large kernel with  $7 \times 7$  spatial size by default.

Table 5: The influence of the depthwise convolution kernel size. We report the performance of Win-Tiny on ImageNet-1K dataset.

| kernel size  | Params. (M) | FLOPs (G) | Top-1 Acc. (%) |
|--------------|-------------|-----------|----------------|
| $3 \times 3$ | 28.33       | 4.51      | 82.2           |
| $5 \times 5$ | 28.36       | 4.52      | 82.2           |
| $7 \times 7$ | 28.50       | 4.56      | 82.3           |

**The influence of the positional encoding.** We attempt different types of positional encoding, including the relative positional encoding (RPE) used in Swin and locally-enhanced positional encoding (LEPE) in CSWin. In fact, RPE is equivalent to a  $7 \times 7$  depthwise convolution with zero padding. In contrast, LEPE is implemented by a  $3 \times 3$  depthwise convolution.

Table 6: The influence of the positional encoding. We report the top-1 classification accuracy of Win-Tiny and Win-Small on ImageNet-1K dataset.

| Model | RPE   | LEPE  | w/o PE |
|-------|-------|-------|--------|
| Win-T | 82.33 | 82.30 | 82.22  |
| Win-S | 83.75 | 83.67 | 83.55  |

As shown in Table 6, RPE achieves slightly higher recognition accuracy than LEPE for both Win-Tiny and Win-Small models. The higher accuracy might be attributed to the larger receptive field of RPE. In the meanwhile, we also testify the performance of our Win without position coding (w/o PE). Table 6 illustrates that, after removing the positional encoding, the performance of the proposed Win becomes slightly worse, but its accuracy is still satisfactory. This is might be due to the fact that the  $7 \times 7$  depthwise convolution we plug after the window-based self-attention module originally developed for achieving cross-window communications simultaneously has the capability of encoding the positional information. Despite that RPE achieves a slightly better performance than LEPE in ImageNet1K image recognition, we set LEPE as the default positional encoding approach since it performs better in the downstream tasks.

## 4.2 Semantic segmentation

**Dataset.** We evaluate the performance of the proposed Win in semantic segmentation on a widely used public benchmark, ADE20K (Zhou et al., 2017). It consists of 20,210 images for training, 2,000 images for validation, and 3,352 images for testing. Following the exiting works, we use the training

images to train our models and report the performance on the validation images. In testing, we report the experimental results of models using the evaluation metric, mIoU, under single-scale (SS) and multi-scale (MS) settings. In the SS setting, the scale of testing images is the same as that of the training images. In contrast, the MS setting adopts scales that are  $[0.5, 0.75, 1.0, 1.25, 1.5, 1.75] \times$  of that for training.

**Setting.** We load the models pre-trained on ImageNet-1K dataset and fine-tune them on the semantic segmentation. To compare with the existing state-of-the-art Vision Transformers in a fair manner, we also adopt UpperNet (Xiao et al., 2018) as the framework for segmentation. Following Swin, in training, we employ the AdamW (Loshchilov and Hutter, 2019) optimizer. The initial learning rate is set as  $6 \times 10^{-5}$ . The weight decay is 0.01. We adopt a scheduler that uses linear learning rate decay. We use a linear warmup with 1,500 iterations. We set the batch size as 16 equally divided into 8 GPU cards. All the models are trained with input size  $512 \times 512$ . The whole training process lasts for 160 thousand iterations. In training, we adopt multiple data augmentation methods, including random horizontal flipping, random re-scaling within ratio range  $[0.5, 2.0]$ , and random photometric distortion. We set the stochastic depth with a ratio of 0.2 for all Win Transformer models.

**Comparisons with state-of-the-art models.** To demonstrate the excellence of the proposed Win Transformer in Semantic Segmentation, we compare it with several state-of-the-art models including Twins (Chu et al., 2021), CSWin Transformer (Dong et al., 2021), Shuffle Transformer (Huang et al., 2021), Focal Transformer (Yang et al., 2021), and Swin Transformer (Liu et al., 2021). As shown in Table 7, our Win Transforms have achieved competitive performance in ADE20K semantic segmentation compared with these state-of-the-art models. To be specific, our Win Transformer consistently outperforms Swin Transformer for tiny, small and base models on both SS and MS settings. Meanwhile, on the SS setting, our Win-S outperforms Twins-B and Focal-S, achieving the second-best performance among all the small-scale models. Moreover, on the SS and MS settings, our Win-B outperforms all compared models except the CSWin-B model and achieves the second-best performance among all the medium-scale models. Again, we emphasize that our Win Transformer is much simpler and easier for implementation than the compared Vision Transformers. The proposed Win Transformer does not need any sophisticated operations but achieves excellent performance in semantic segmentation.

**The influence of the positional encoding.** We compare the performance of the relative positional encoding (RPE) and the locally-enhanced positional encoding (LEPE) on semantic segmentation. As shown in Table 8, using LEPE, Win-T as well as Win-S model achieve a better performance in semantic segmentation. As we mentioned previously, compared with RPE, LEPE has a smaller receptive field, which might be helpful for semantic segmentation where the local context is critical. By default, we adopt LEPE method.

### 4.3 Object detection and instance segmentation

**Dataset.** We evaluate the object detection and instance segmentation on MS-COCO 2017 public benchmark (Lin et al., 2014), consisting of 118 thousand training images, 5 thousand validation images, and 20 thousand test-dev images. We pre-train the backbones on the ImageNet-1K dataset and then fine-tune the pre-trained model on the MS-COCO 2017 training set.

**Settings.** We adopt Mask-RCNN (He et al., 2017) as the object detection framework. Following Swin Transformer, we conduct multi-scale training, which resizes the input image such that the shorter side is larger than 480 and smaller than 800 while the longer side is not larger than 1333.

Table 7: Comparisons with the state-of-the-art convolutional neural networks and Vision Transformers on ADE20K semantic segmentation. FLOPs is measured on the input image of  $1024 \times 1024$  resolution. SS denotes the single-scale setting and MS denotes the multi-scale setting.

| Method                         | Params. (M) | FLOPs (G) | SS mIoU (%) | MS mIoU (%) |
|--------------------------------|-------------|-----------|-------------|-------------|
| ConvNeXt-T (Liu et al., 2022)  | 60          | 939       | -           | 46.7        |
| TwinsP-S (Chu et al., 2021)    | 55          | 919       | 46.2        | 47.5        |
| Twins-S (Chu et al., 2021)     | 54          | 901       | 46.2        | 47.1        |
| CSWin-T (Dong et al., 2021)    | 60          | 959       | 49.3        | 50.4        |
| Shuffle-T (Huang et al., 2021) | 60          | 949       | 46.6        | 47.6        |
| Focal-T (Yang et al., 2021)    | 62          | 998       | 45.8        | 47.0        |
| Swin-T (Dong et al., 2021)     | 60          | 945       | 44.5        | 45.8        |
| Win-T (ours)                   | 60          | 949       | 45.7        | 47.2        |
| ConvNeXt-S (Liu et al., 2022)  | 82          | 1027      | -           | 49.6        |
| TwinsP-B (Chu et al., 2021)    | 74          | 977       | 47.1        | 48.4        |
| Twins-B (Chu et al., 2021)     | 89          | 1020      | 47.7        | 48.9        |
| CSWin-S (Dong et al., 2021)    | 65          | 1027      | 50.4        | 50.8        |
| Shuffle-S (Huang et al., 2021) | 81          | 1044      | 48.4        | 49.6        |
| Focal-S (Yang et al., 2021)    | 85          | 1130      | 48.0        | 50.0        |
| Swin-S (Dong et al., 2021)     | 81          | 1038      | 47.6        | 49.4        |
| Win-S (ours)                   | 81          | 1044      | 48.4        | 49.8        |
| ConvNeXt-B (Liu et al., 2022)  | 122         | 1170      | -           | 49.9        |
| TwinsP-L (Chu et al., 2021)    | 92          | 1041      | 48.6        | 49.8        |
| Twins-L (Chu et al., 2021)     | 133         | 1164      | 48.8        | 50.2        |
| CSWin-B (Dong et al., 2021)    | 109         | 1222      | 51.1        | 51.7        |
| Shuffle-B (Huang et al., 2021) | 121         | 1196      | 49.0        | 50.5        |
| Focal-B (Yang et al., 2021)    | 126         | 1354      | 49.0        | 50.5        |
| Swin-B (Dong et al., 2021)     | 121         | 1188      | 48.1        | 49.7        |
| Win-B (ours)                   | 121         | 1196      | 49.2        | 50.7        |

Table 8: The influence of the positional encoding on ADE20K semantic segmentation. We report the mIoU on single-scale and multi-scale settings.

|       | RPE     |         | LEPE    |         |
|-------|---------|---------|---------|---------|
|       | SS mIoU | MS mIoU | SS mIoU | MS mIoU |
| Win-T | 45.3    | 46.9    | 45.7    | 47.2    |
| Win-S | 48.0    | 49.6    | 48.4    | 49.8    |

We adopt a  $3\times$  schedule with 36 epochs in total and decay the learning rate to 0.1 at the 27th epoch and the 33th epoch. We adopt AdamW optimizer and set the initial learning rate as 0.0001, weight decay as 0.05, and batch size as 16. We use 8 GPU cards for training. We set the stochastic depth ratio as 0.2 for all Win Transformer models.

Table 9: Comparisons with convolutional neural networks and Vision Transformers based on Mask-RCNN framework on MSCOCO-2017 object detection and instance segmentation. FLOPs is evaluated on  $1280 \times 800$  resolution.  $AP^b$  denotes the box-level average precision for evaluating the performance of object detection and  $AP^m$  denotes the mask-level average precision for instance segmentation.

| Method                           | Params | FLOPs | $AP^b$ | $AP_{50}^b$ | $AP_{75}^b$ | $AP^m$ | $AP_{50}^m$ | $AP_{75}^m$ |
|----------------------------------|--------|-------|--------|-------------|-------------|--------|-------------|-------------|
| ResNet-50 (He et al., 2016)      | 44 M   | 260 G | 41.0   | 61.7        | 44.9        | 37.1   | 58.4        | 40.1        |
| ConvNeXt-T (Liu et al., 2022)    | 48 M   | 262 G | 46.2   | 67.9        | 50.8        | 41.7   | 65.0        | 44.9        |
| PVT-S (Wang et al., 2021)        | 44 M   | 256 G | 43.0   | 65.3        | 46.9        | 39.9   | 62.5        | 42.8        |
| ViL-S (Zhang et al., 2021)       | 45 M   | 218 G | 47.1   | 68.7        | 51.5        | 42.7   | 65.9        | 46.2        |
| TwinsP-S (Chu et al., 2021)      | 44 M   | 245 G | 46.8   | 69.3        | 51.8        | 42.6   | 66.3        | 46.0        |
| Twins-S (Chu et al., 2021)       | 44 M   | 228 G | 46.8   | 69.2        | 51.2        | 42.6   | 66.3        | 45.8        |
| CSWin-T (Dong et al., 2021)      | 42 M   | 279 G | 49.0   | 70.7        | 53.7        | 43.6   | 67.9        | 46.6        |
| Shuffle-T (Huang et al., 2021)   | 48 M   | 268 G | 46.8   | 68.9        | 51.5        | 42.3   | 66.0        | 45.6        |
| Focal-T (Yang et al., 2021)      | 49 M   | 291 G | 47.2   | 69.4        | 51.9        | 42.7   | 66.5        | 45.9        |
| Swin-T (Dong et al., 2021)       | 48 M   | 264 G | 46.0   | 68.2        | 50.2        | 41.6   | 65.1        | 44.8        |
| Win-T (ours)                     | 48 M   | 268 G | 46.6   | 68.4        | 51.1        | 42.1   | 65.7        | 45.3        |
| ResNet-101 (He et al., 2016)     | 63 M   | 336 G | 42.8   | 63.2        | 47.1        | 38.5   | 60.1        | 41.3        |
| PVT-M (Wang et al., 2021)        | 64 M   | 302 G | 44.2   | 66.0        | 48.2        | 40.5   | 63.1        | 43.5        |
| ViL-M (Zhang et al., 2021)       | 60 M   | 261 G | 44.6   | 66.3        | 48.5        | 40.7   | 63.8        | 43.7        |
| TwinsP-B (Chu et al., 2021)      | 64 M   | 302 G | 47.9   | 70.1        | 52.5        | 43.2   | 67.2        | 46.3        |
| Twins-B (Chu et al., 2021)       | 76 M   | 340 G | 48.0   | 69.5        | 52.7        | 43.0   | 66.8        | 46.6        |
| CSWin-S (Dong et al., 2021)      | 54 M   | 342 G | 50.0   | 71.3        | 54.7        | 44.5   | 68.4        | 47.7        |
| Shuffle-S (Huang et al., 2021)   | 69 M   | 359 G | 48.4   | 70.1        | 53.5        | 43.3   | 67.3        | 46.7        |
| Focal-S (Yang et al., 2021)      | 71 M   | 401 G | 48.8   | 70.5        | 53.6        | 43.8   | 67.7        | 47.2        |
| Swin-S (Dong et al., 2021)       | 69 M   | 354 G | 48.5   | 70.2        | 53.5        | 43.3   | 67.3        | 46.6        |
| Win-S (ours)                     | 69 M   | 359 G | 48.6   | 69.8        | 53.3        | 43.4   | 67.3        | 46.7        |
| ResNeXt101-64 (Xie et al., 2017) | 101 M  | 493 G | 44.4   | 64.9        | 48.8        | 39.7   | 61.9        | 42.6        |
| PVT-L (Wang et al., 2021)        | 81 M   | 364 G | 44.5   | 66.0        | 48.3        | 40.7   | 63.4        | 43.7        |
| ViL-B (Zhang et al., 2021)       | 76 M   | 365 G | 45.7   | 67.2        | 49.9        | 41.3   | 64.4        | 44.5        |
| CSWin-B (Dong et al., 2021)      | 97 M   | 526 G | 50.8   | 72.1        | 55.8        | 44.9   | 69.1        | 48.3        |
| Focal-B (Yang et al., 2021)      | 110 M  | 533 G | 49.0   | 70.1        | 53.6        | 43.7   | 67.6        | 47.0        |
| Swin-B (Dong et al., 2021)       | 107 M  | 496 G | 48.5   | 69.8        | 53.2        | 43.4   | 66.8        | 46.9        |
| Win-B (ours)                     | 108 M  | 503 G | 49.1   | 70.2        | 53.8        | 43.8   | 67.8        | 47.1        |

**Comparisons with state-of-the-art methods.** To demonstrate the outstanding performance of the proposed Win Transformers on object detection and instance segmentation, we compare them with convolutional neural networks including ResNet (He et al., 2016), ResNeXt (Xie et al., 2017) and ConvNeXt (Liu et al., 2022). Meanwhile, we also compare them with other Vision Transformers including PVT (Wang et al., 2021), ViL (Zhang et al., 2021), Twins (Chu et al., 2021), CSWin (Dong et al., 2021), Shuffle Transformer (Huang et al., 2021), Focal Transformer (Yang et al., 2021) and Swin Transformer (Liu et al., 2021). As shown in Table 9, the proposed Win-T consistently outperform the recent state-of-the-art convolutional neural network (ConvNeXt-T) and Swin-T. In the meanwhile, our Win-S further outperforms PVT-M, ViL-M, TwinsP-B, Shuffle-S,

and Swin-B. Moreover, our Win-B achieves the second-best performance among all medium-size Vision Transformers. Note that the proposed Win Transformer is much conceptually simpler than the compared Vision Transformers, and thus, its implementation is much easier. The competitive effectiveness, high efficiency, and attractive simplicity make the proposed Win Transformer a good choice in real applications.

## 5 Conclusions

Vision Transformers suffer from the efficiency issue caused by the quadratic computational complexity of self-attention operations with respect to the token number. To achieve a good trade-off between effectiveness and efficiency, some following works such as Swin Transformer adopt window-based local attention mechanism. They exploit the self-attention operations within each local window and attempt to achieve the cross-window communications through varying the window partitioning through several sophisticated operations, which brings difficulty in implementation. In this work, we attempt to achieve cross-window communication through a depthwise convolution and check the necessity of these sophisticated operations. Our experiments show that a simple depthwise convolution is sufficiently effective to achieve cross-window communications. With the existence of depthwise convolution, the shifted window partitioning can not bring additional performance improvement. Thus, we remove the most innovative part in the Swin Transformer and degenerate the Swin Transformer to the proposed Win Transformer. To demonstrate the excellence of the proposed Win Transformers, we conduct systematic experiments on multiple computer vision tasks including image recognition, semantic segmentation and object detection. The experimental results on multiple public benchmarks demonstrate the attractive effectiveness and efficiency of the proposed Win Transformers.

## References

- Jimmy Lei Ba, Jamie Ryan Kiros, and Geoffrey E Hinton. Layer normalization. *arXiv preprint arXiv:1607.06450*, 2016.
- Irwan Bello, Barret Zoph, Quoc Le, Ashish Vaswani, and Jonathon Shlens. Attention augmented convolutional networks. In *Proceedings of the 2019 IEEE/CVF International Conference on Computer Vision (ICCV)*, pages 3285–3294, Seoul, Korea, 2019.
- Yue Cao, Jiarui Xu, Stephen Lin, Fangyun Wei, and Han Hu. Gcnet: Non-local networks meet squeeze-excitation networks and beyond. In *Proceedings of the IEEE/CVF International Conference on Computer Vision Workshops*, 2019.
- Nicolas Carion, Francisco Massa, Gabriel Synnaeve, Nicolas Usunier, Alexander Kirillov, and Sergey Zagoruyko. End-to-end object detection with transformers. In *Computer Vision - ECCV 2020 - Proceedings of the 16th European Conference on Computer Vision (ECCV), Part I*, pages 213–229, Glasgow, UK, 2020.
- Shuo Chen, Tan Yu, and Ping Li. MVT: multi-view vision transformer for 3D object recognition. In *Proceedings of the 32nd British Machine Vision Conference (BMVC)*, page 349, Online, 2021.
- Cheng Chi, Fangyun Wei, and Han Hu. RelationNet++: Bridging visual representations for object detection via transformer decoder. In *Advances in Neural Information Processing Systems (NeurIPS)*, virtual, 2020.

- Xiangxiang Chu, Zhi Tian, Yuqing Wang, Bo Zhang, Haibing Ren, Xiaolin Wei, Huaxia Xia, and Chunhua Shen. Twins: Revisiting the design of spatial attention in vision transformers. In *Advances in Neural Information Processing Systems (NeurIPS)*, pages 9355–9366, virtual, 2021.
- Ekin D Cubuk, Barret Zoph, Jonathon Shlens, and Quoc V Le. Randaugment: Practical automated data augmentation with a reduced search space. In *Proceedings of the IEEE/CVF Conference on Computer Vision and Pattern Recognition Workshops*, pages 702–703, 2020.
- Khoa Doan, Yingjie Lao, and Ping Li. Backdoor attack with imperceptible input and latent modification. In *Advances in Neural Information Processing Systems (NeurIPS)*, pages 18944–18957, virtual, 2021a.
- Khoa Doan, Yingjie Lao, Weijie Zhao, and Ping Li. LIRA: learnable, imperceptible and robust backdoor attacks. In *Proceedings of the 2021 IEEE/CVF International Conference on Computer Vision (ICCV)*, pages 11946–11956, Montreal, Canada, 2021b.
- Khoa D Doan, Yingjie Lao, Peng Yang, and Ping Li. Defending backdoor attacks on vision transformer via patch processing. *arXiv preprint arXiv:2206.12381*, 2022.
- Xiaoyi Dong, Jianmin Bao, Dongdong Chen, Weiming Zhang, Nenghai Yu, Lu Yuan, Dong Chen, and Baining Guo. Cswin transformer: A general vision transformer backbone with cross-shaped windows, 2021.
- Alexey Dosovitskiy, Lucas Beyer, Alexander Kolesnikov, Dirk Weissenborn, Xiaohua Zhai, Thomas Unterthiner, Mostafa Dehghani, Matthias Minderer, Georg Heigold, Sylvain Gelly, Jakob Uszkoreit, and Neil Houlsby. An image is worth 16x16 words: Transformers for image recognition at scale. In *Proceedings of the 9th International Conference on Learning Representations (ICLR)*, Virtual Event, Austria, 2021.
- Haoqi Fan, Bo Xiong, Karttikeya Mangalam, Yanghao Li, Zhicheng Yan, Jitendra Malik, and Christoph Feichtenhofer. Multiscale vision transformers. In *Proceedings of the 2021 IEEE/CVF International Conference on Computer Vision (ICCV)*, pages 6804–6815, Montreal, Canada, 2021.
- Benjamin Graham, Alaaeldin El-Nouby, Hugo Touvron, Pierre Stock, Armand Joulin, Hervé Jégou, and Matthijs Douze. Levit: a vision transformer in convnet’s clothing for faster inference. In *Proceedings of the IEEE/CVF International Conference on Computer Vision*, pages 12259–12269, 2021.
- Kai Han, Yunhe Wang, Hanting Chen, Xinghao Chen, Jianyuan Guo, Zhenhua Liu, Yehui Tang, An Xiao, Chunjing Xu, Yixing Xu, Zhaohui Yang, Yiman Zhang, and Dacheng Tao. A survey on visual transformer. *arXiv preprint arXiv:2012.12556*.
- Kai Han, An Xiao, Enhua Wu, Jianyuan Guo, Chunjing Xu, and Yunhe Wang. Transformer in transformer. In *Advances in Neural Information Processing Systems (NeurIPS)*, pages 15908–15919, virtual, 2021a.
- Qi Han, Zejia Fan, Qi Dai, Lei Sun, Ming-Ming Cheng, Jiaying Liu, and Jingdong Wang. Demystifying local vision transformer: Sparse connectivity, weight sharing, and dynamic weight. *arXiv preprint arXiv:2106.04263*, 2021b.
- Kaiming He, Xiangyu Zhang, Shaoqing Ren, and Jian Sun. Deep residual learning for image recognition. In *Proceedings of the 2016 IEEE Conference on Computer Vision and Pattern Recognition (CVPR)*, pages 770–778, Las Vegas, NV, 2016.

- Kaiming He, Georgia Gkioxari, Piotr Dollár, and Ross B. Girshick. Mask R-CNN. In *Proceedings of the IEEE International Conference on Computer Vision (ICCV)*, pages 2980–2988, Venice, Italy, 2017.
- Byeongho Heo, Sangdoon Yun, Dongyoon Han, Sanghyuk Chun, Junsuk Choe, and Seong Joon Oh. Rethinking spatial dimensions of vision transformers. In *Proceedings of the 2021 IEEE/CVF International Conference on Computer Vision (ICCV)*, pages 11916–11925, Montreal, Canada, 2021.
- Elad Hoffer, Tal Ben-Nun, Itay Hubara, Niv Giladi, Torsten Hoefler, and Daniel Soudry. Augment your batch: Improving generalization through instance repetition. In *Proceedings of the 2020 IEEE/CVF Conference on Computer Vision and Pattern Recognition (CVPR)*, pages 8126–8135, Seattle, WA, 2020.
- Gao Huang, Yu Sun, Zhuang Liu, Daniel Sedra, and Kilian Q. Weinberger. Deep networks with stochastic depth. In *Proceedings of the 14th European Conference on Computer Vision (ECCV)*, pages 646–661, Amsterdam, The Netherlands, Part IV, 2016.
- Zilong Huang, Yucheng Ben, Guozhong Luo, Pei Cheng, Gang Yu, and Bin Fu. Shuffle transformer: Rethinking spatial shuffle for vision transformer. *arXiv preprint arXiv:2106.03650*, 2021.
- Alex Krizhevsky, Ilya Sutskever, and Geoffrey E. Hinton. ImageNet classification with deep convolutional neural networks. In *Advances in Neural Information Processing Systems (NIPS)*, pages 1106–1114, Lake Tahoe, NV, 2012.
- Yann LeCun, Yoshua Bengio, et al. Convolutional networks for images, speech, and time series. *The handbook of brain theory and neural networks*, 3361(10):1995, 1995.
- Kunchang Li, Yali Wang, Peng Gao, Guanglu Song, Yu Liu, Hongsheng Li, and Yu Qiao. UniFormer: Unified transformer for efficient spatiotemporal representation learning. *arXiv preprint arXiv:2201.04676*, 2022.
- Tsung-Yi Lin, Michael Maire, Serge J. Belongie, James Hays, Pietro Perona, Deva Ramanan, Piotr Dollár, and C. Lawrence Zitnick. Microsoft COCO: common objects in context. In *Computer Vision - ECCV 2014 - Proceedings of the 13th European Conference on Computer Vision (ECCV), Part V*, pages 740–755, Zurich, Switzerland, 2014.
- Ze Liu, Yutong Lin, Yue Cao, Han Hu, Yixuan Wei, Zheng Zhang, Stephen Lin, and Baining Guo. Swin transformer: Hierarchical vision transformer using shifted windows. In *Proceedings of the 2021 IEEE/CVF International Conference on Computer Vision (ICCV)*, pages 9992–10002, Montreal, Canada, 2021.
- Zhuang Liu, Hanzi Mao, Chao-Yuan Wu, Christoph Feichtenhofer, Trevor Darrell, and Saining Xie. A convnet for the 2020s. In *Proceedings of the IEEE/CVF Conference on Computer Vision and Pattern Recognition (CVPR)*, New Orleans, LA, 2022.
- Ilya Loshchilov and Frank Hutter. Decoupled weight decay regularization. In *Proceedings of the 7th International Conference on Learning Representations (ICLR)*, New Orleans, LA, 2019.
- Zizheng Pan, Bohan Zhuang, Jing Liu, Haoyu He, and Jianfei Cai. Scalable vision transformers with hierarchical pooling. In *Proceedings of the 2021 IEEE/CVF International Conference on Computer Vision (ICCV)*, pages 367–376, Montreal, Canada, 2021.

- Zizheng Pan, Bohan Zhuang, Haoyu He, Jing Liu, and Jianfei Cai. Less is more: Pay less attention in vision transformers. In *Proceedings of the Thirty-Sixth AAAI Conference on Artificial Intelligence (AAAI)*, pages 2035–2043, Virtual Event, 2022.
- Boris T Polyak and Anatoli B Juditsky. Acceleration of stochastic approximation by averaging. *SIAM J. Control. Optim.*, 30(4):838–855, 1992.
- Ilija Radosavovic, Raj Prateek Kosaraju, Ross B. Girshick, Kaiming He, and Piotr Dollár. Designing network design spaces. In *Proceedings of the 2020 IEEE/CVF Conference on Computer Vision and Pattern Recognition (CVPR)*, pages 10425–10433, Seattle, WA, 2020.
- Aravind Srinivas, Tsung-Yi Lin, Niki Parmar, Jonathon Shlens, Pieter Abbeel, and Ashish Vaswani. Bottleneck transformers for visual recognition. In *Proceedings of the IEEE Conference on Computer Vision and Pattern Recognition (CVPR)*, pages 16519–16529, virtual, 2021.
- Hugo Touvron, Matthieu Cord, Matthijs Douze, Francisco Massa, Alexandre Sablayrolles, and Hervé Jégou. Training data-efficient image transformers & distillation through attention. In *Proceedings of the 38th International Conference on Machine Learning (ICML)*, pages 10347–10357, Virtual Event, 2021a.
- Hugo Touvron, Matthieu Cord, Alexandre Sablayrolles, Gabriel Synnaeve, and Hervé Jégou. Going deeper with image transformers. In *Proceedings of the 2021 IEEE/CVF International Conference on Computer Vision (ICCV)*, pages 32–42, Montreal, Canada, 2021b.
- Ashish Vaswani, Noam Shazeer, Niki Parmar, Jakob Uszkoreit, Llion Jones, Aidan N Gomez, Łukasz Kaiser, and Illia Polosukhin. Attention is all you need. In *Advances in Neural Information Processing Systems (NIPS)*, pages 5998–6008, Long Beach, CA, 2017.
- Wenhai Wang, Enze Xie, Xiang Li, Deng-Ping Fan, Kaitao Song, Ding Liang, Tong Lu, Ping Luo, and Ling Shao. Pyramid vision transformer: A versatile backbone for dense prediction without convolutions. In *Proceedings of the 2021 IEEE/CVF International Conference on Computer Vision (ICCV)*, pages 548–558, Montreal, Canada, 2021.
- Wenxiao Wang, Lu Yao, Long Chen, Binbin Lin, Deng Cai, Xiaofei He, and Wei Liu. CrossFormer: A versatile vision transformer hinging on cross-scale attention. In *Proceedings of the Tenth International Conference on Learning Representations (ICLR)*, Virtual Event, 2022.
- Xiaolong Wang, Ross B. Girshick, Abhinav Gupta, and Kaiming He. Non-local neural networks. In *Proceedings of the 2018 IEEE Conference on Computer Vision and Pattern Recognition (CVPR)*, pages 7794–7803, Salt Lake City, UT, 2018.
- Haiping Wu, Bin Xiao, Noel Codella, Mengchen Liu, Xiyang Dai, Lu Yuan, and Lei Zhang. CvT: Introducing convolutions to vision transformers. In *Proceedings of the 2021 IEEE/CVF International Conference on Computer Vision (ICCV)*, pages 22–31, Montreal, Canada, 2021.
- Tete Xiao, Yingcheng Liu, Bolei Zhou, Yuning Jiang, and Jian Sun. Unified perceptual parsing for scene understanding. In *Proceedings of the 15th European Conference on Computer Vision (ECCV), Part V*, pages 432–448, Munich, Germany, 2018.
- Tete Xiao, Mannat Singh, Eric Mintun, Trevor Darrell, Piotr Dollár, and Ross B. Girshick. Early convolutions help transformers see better. In *Advances in Neural Information Processing Systems (NeurIPS)*, pages 30392–30400, virtual, 2021.

- Enze Xie, Wenhai Wang, Zhiding Yu, Anima Anandkumar, Jose M. Alvarez, and Ping Luo. SegFormer: Simple and efficient design for semantic segmentation with transformers. In *Advances in Neural Information Processing Systems (NeurIPS)*, pages 12077–12090, virtual, 2021.
- Saining Xie, Ross B. Girshick, Piotr Dollár, Zhuowen Tu, and Kaiming He. Aggregated residual transformations for deep neural networks. In *Proceedings of the 2017 IEEE Conference on Computer Vision and Pattern Recognition (CVPR)*, pages 5987–5995, Honolulu, HI, 2017.
- Jianwei Yang, Chunyuan Li, Pengchuan Zhang, Xiyang Dai, Bin Xiao, Lu Yuan, and Jianfeng Gao. Focal attention for long-range interactions in vision transformers. In *Advances in Neural Information Processing Systems (NeurIPS)*, pages 30008–30022, virtual, 2021.
- Minghao Yin, Zhuliang Yao, Yue Cao, Xiu Li, Zheng Zhang, Stephen Lin, and Han Hu. Disentangled non-local neural networks. In Andrea Vedaldi, Horst Bischof, Thomas Brox, and Jan-Michael Frahm, editors, *Proceedings of the 16th European Conference on Computer Vision (ECCV), Part XV*, pages 191–207, 2020.
- Tan Yu, Yi Yang, Yi Li, Xiaodong Chen, Mingming Sun, and Ping Li. Combo-attention network for baidu video advertising. In *Proceedings of the 26th ACM SIGKDD Conference on Knowledge Discovery and Data Mining (KDD)*, pages 2474–2482, Virtual Event, CA, 2020.
- Tan Yu, Xuemeng Yang, Yan Jiang, Hongfang Zhang, Weijie Zhao, and Ping Li. TIRA in Baidu image advertising. In *Proceedings of the 37th IEEE International Conference on Data Engineering (ICDE)*, pages 2207–2212, Chania, Greece, 2021a.
- Tan Yu, Yi Yang, Yi Li, Lin Liu, Hongliang Fei, and Ping Li. Heterogeneous attention network for effective and efficient cross-modal retrieval. In *Proceedings of the 44th International ACM SIGIR Conference on Research and Development in Information Retrieval (SIGIR)*, pages 1146–1156, Virtual Event, Canada, 2021b.
- Tan Yu, Zhipeng Jin, Jie Liu, Yi Yang, Hongliang Fei, and Ping Li. Boost CTR prediction for new advertisements via modeling visual content. *arXiv preprint arXiv:2209.11727*, 2022a.
- Tan Yu, Gangming Zhao, Ping Li, and Yizhou Yu. BOAT: Bilateral local attention vision transformer. In *Proceedings of the 33rd British Machine Vision Conference (BMVC)*, London, UK, 2022b.
- Li Yuan, Yunpeng Chen, Tao Wang, Weihao Yu, Yujun Shi, Zihang Jiang, Francis E. H. Tay, Jiashi Feng, and Shuicheng Yan. Tokens-to-Token ViT: Training vision transformers from scratch on ImageNet. In *Proceedings of the 2021 IEEE/CVF International Conference on Computer Vision (ICCV)*, pages 538–547, Montreal, Canada, 2021.
- Sangdoon Yun, Dongyoon Han, Sanghyuk Chun, Seong Joon Oh, Youngjoon Yoo, and Junsuk Choe. CutMix: Regularization strategy to train strong classifiers with localizable features. In *Proceedings of the 2019 IEEE/CVF International Conference on Computer Vision (ICCV)*, pages 6022–6031, 2019.
- Hongyi Zhang, Moustapha Cissé, Yann N. Dauphin, and David Lopez-Paz. mixup: Beyond empirical risk minimization. In *Proceedings of the 6th International Conference on Learning Representations (ICLR)*, Vancouver, Canada, 2018.
- Pengchuan Zhang, Xiyang Dai, Jianwei Yang, Bin Xiao, Lu Yuan, Lei Zhang, and Jianfeng Gao. Multi-scale vision longformer: A new vision transformer for high-resolution image encoding. In

- Proceedings of the 2021 IEEE/CVF International Conference on Computer Vision (ICCV)*, pages 2978–2988, Montreal, Canada, 2021.
- Zizhao Zhang, Han Zhang, Long Zhao, Ting Chen, Sercan Ö. Arik, and Tomas Pfister. Nested hierarchical transformer: Towards accurate, data-efficient and interpretable visual understanding. In *Proceedings of the thirty-Sixth AAAI Conference on Artificial Intelligence (AAAI)*, pages 3417–3425, Virtual Event, 2022.
- Sixiao Zheng, Jiachen Lu, Hengshuang Zhao, Xiatian Zhu, Zekun Luo, Yabiao Wang, Yanwei Fu, Jianfeng Feng, Tao Xiang, Philip H. S. Torr, and Li Zhang. Rethinking semantic segmentation from a sequence-to-sequence perspective with transformers. In *Proceedings of the IEEE Conference on Computer Vision and Pattern Recognition (CVPR)*, pages 6881–6890, virtual, 2021.
- Zhun Zhong, Liang Zheng, Guoliang Kang, Shaozi Li, and Yi Yang. Random erasing data augmentation. In *Proceedings of the Thirty-Fourth AAAI Conference on Artificial Intelligence (AAAI)*, pages 13001–13008, New York, NY, 2020.
- Bolei Zhou, Hang Zhao, Xavier Puig, Sanja Fidler, Adela Barriuso, and Antonio Torralba. Scene parsing through ADE20K dataset. In *Proceedings of the 2017 IEEE Conference on Computer Vision and Pattern Recognition (CVPR)*, pages 5122–5130, Honolulu, HI, 2017.
- Daquan Zhou, Bingyi Kang, Xiaojie Jin, Linjie Yang, Xiaochen Lian, Zihang Jiang, Qibin Hou, and Jiashi Feng. DeepViT: Towards deeper vision transformer. *arXiv preprint arXiv:2103.11886*, 2021.
- Xizhou Zhu, Weijie Su, Lewei Lu, Bin Li, Xiaogang Wang, and Jifeng Dai. Deformable DETR: deformable transformers for end-to-end object detection. In *Proceedings of the 9th International Conference on Learning Representations (ICLR)*, Virtual Event, Austria, 2021.